METHANE PLUMES DETECTION ON PRISMA L1 IMAGES WITH THE ADJUSTED SPECTRAL MATCHED FILTER AND WIND DATA

E. Ouerghi, T. Ehret, Gabriele Facciolo, E. Meinhardt, J.-M. Morel, C. de Franchis, T. Lauvaux

METHANE PLUMES DETECTION ON PRISMA L1 IMAGES WITH THE ADJUSTED SPECTRAL MATCHED FILTER AND WIND DATA

E. Ouerghi, T. Ehret, G. Facciolo
E. Meinhardt, J.-M. Morel

Université Paris-Saclay, CNRS
ENS Paris-Saclay, Centre Borelli, France

C. de Franchis[†]
T. Lauvaux[‡]

[†]Kayrros SAS, France
[‡]GSMA, University of Reims

ABSTRACT

Reducing methane emissions is essential to tackle climate change. Here, we address the problem of detecting automatically point source methane leaks using high resolution hyperspectral images from the PRISMA satellite. We use a variation of the Matched Filter (MF) called the Adjusted Spectral Matched Filter (ASMF) to detect methane plumes in satellite images. To remove false positives, the detected plumes are confirmed by comparing their orientation to the wind direction extracted from the standard meteorological reanalysis product ERA5. The ASMF reduces the fraction of false detections compared to the MF and without preventing the detection of plumes. To validate the method, we use a recently proposed dataset of manually annotated plumes on PRISMA images. We also compare our detection rate to the detection rate of methods using deep learning or the standard matched filter. We then show that our method outperforms those methods in terms of F1 score.

***Index Terms*—** Hyperspectral images, Matched filter, Wind data, Methane, Anomaly detection

1. INTRODUCTION

The detection of methane (CH_4) leaks from anthropogenic activities is a cost-effective and global approach, which could help rapidly reducing greenhouse gas (GHG) emissions. In a time lapse of 20 years, a CH_4 molecule has a global warming potential 80 times larger than carbon dioxide (CO_2) [1]. A significant part of human CH_4 emissions could be reduced or fully-avoided, as about 33% come from oil and gas infrastructures.

These methane emissions are usually "point emissions", which means that the plume is emitted from a small surface on the ground but contains a large amount of gas. The detection of these emissions therefore requires instruments capable of observing the whole globe at high spatial resolutions.

Work partly financed by Office of Naval research grant N00014-20-S-B001, MENRT, and a PhD scholarship financed by MESRI (Ministère de l'Enseignement Supérieur, de la Recherche et de l'Innovation). Centre Borelli is also a member of Université Paris Cité, SSA and INSERM.

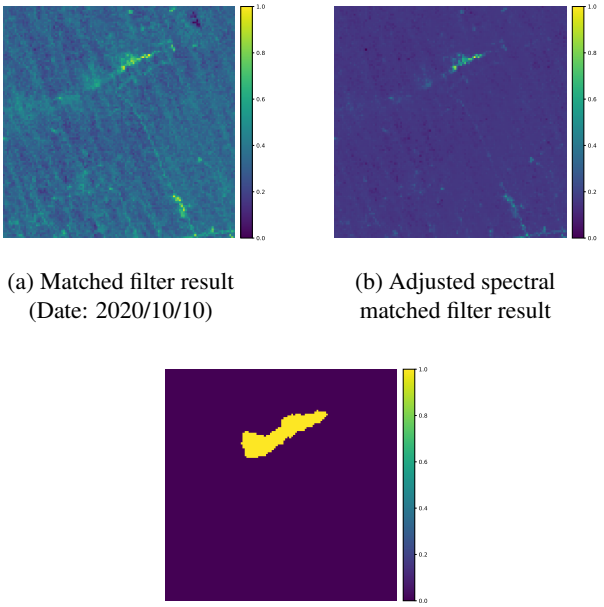

(a) Matched filter result (Date: 2020/10/10)

(b) Adjusted spectral matched filter result

(d) Ground truth

Fig. 1: Comparison between the matched filter and the Adjusted Spectral Matched Filter (ASMF). The tested methane plume is in Turkmenistan.

In order to detect GHG fossil fuel emissions from human activities, several satellites have been placed in orbit around the Earth over the past ten years. Here, we focus on PRISMA [2] (PRecursore IperSpettrale della Missione Applicativa), a satellite launched in 2019 by the Italian Space Agency. PRISMA provides hyperspectral images with a high spatial resolution (30m) and a swath of 30 km. Each pixel contains a spectrum with 237 channels between 400nm and 2500nm.

Methods for the detection of point source methane emissions on PRISMA already exist with in particular the work of [3], which is based on the matched filter algorithm. The work presented in [3] is based on the application of the matched filter and a manual segmentation of the plumes.

Here, we propose an improvement of this method comprising an automatic methane plume detection algorithm involving a variant of the matched filter. Our plume detection algorithm is automatic, unsupervised, and reduces the number of false positives with respect to the standard matched filter. Our method involves two steps: (i) We compute a matched filter variant called the Adjusted Spectral Matched Filter (ASMF) [4], the ASMF highlights the plumes while reducing the number of false positives. (ii) Then, to remove a part of the false positives, we compare the orientation of the plume detected in (ii) with the orientation of the wind.

To validate the method, we evaluate our approach on manually-annotated plumes detected in PRISMA satellite images from a recently-published dataset [5]. We also compare our detection rate to the detection rate of the methods proposed by [5] and [3]. We then show that our method outperforms the methods proposed by [5] and [3] based on a comparison of the F1 score.

2. RELATED WORK

In the context of hyperspectral imagers two main techniques have been applied to detect methane plumes, both aiming at the quantification of the methane concentrations in the observed area.

The first is the Iterative maximum a posteriori applied to differential optical absorption spectroscopy (IMAP-DOAS) [6]. This method consists in inverting a complete atmospheric absorption model with an optimal estimation algorithm. IMAP-DOAS works with sensors that have very different spectral and spatial resolutions, such as AVIRIS [7] and TROPOMI [8]. In the case of TROPOMI, the implementation is based on the work presented in [9].

The second technique is the matched filter. The matched filter is a linear filter that quantifies the presence of an anomaly whose spectral signature is known. The matched filter allows to compute the excess methane concentration with more computational efficiency than the IMAP-DOAS method. However, it only retrieves the concentration of methane whereas the IMAP-DOAS retrieves the concentration of all gases. It is mainly used for the PRISMA satellite [3]. Several matched filter variations exist. One used for methane plume detection is the Cluster-Tuned Matched Filter (CTMF), originally dedicated to sulfur dioxide [10], and then applied to CH_4 plume detection in [11]. Here we focus on another matched filter variant: the adjusted spectral matched filter (ASMF) [4]. The ASMF allows to remove false positives from the matched filter image and therefore has a lower false positive rate than methods like the CTMF, which rely mainly on the improvement of the parameter computation.

3. MATERIALS

We use the level 1 images from the PRISMA satellite. Those images are hyperspectral images with a 30m spatial resolution and contain at each pixel a 237 channels spectrum between 400nm and 2500nm. Here, we are interested in the SWIR region of the spectrum containing 171 channels in a spectral interval of $920 - 2505$nm.

We also use wind data from the ECMWF ERA5 dataset [12]. Wind data are used to compare the orientation of the plume with the orientation of the wind. The ECMWF provides hourly wind data with a spatial resolution of 30km.

Lastly, we use a detailed CH_4 absorption spectrum taken from the HITRAN spectral database [13]. Spectrum variations are small in the near-surface atmospheric layers so we selected the CH_4 spectrum at $15°$C and 1 atm to represent near-surface atmospheric conditions.

4. METHOD

4.1. Adjusted spectral matched filter

The state-of-the-art methods on PRISMA use the standard matched filter to detect methane plumes [3]. For a given pixel x, the matched filter detector $\mathcal{D}_{MF}(x)$ is defined by

$$\mathcal{D}_{MF}(x) = \frac{\mathbf{t}^T \Sigma^{-1}(x-\mu)}{\mathbf{t}^T \Sigma^{-1} \mathbf{t}}, \tag{1}$$

where μ and Σ are the mean and covariance of the background, and $\mathbf{t}$ is the target vector. It represents the direction of the expected perturbation when observing a pixel with a methane plume. In the case of gas detection, the target vector is defined by [14, 3] as

$$\mathbf{t} = -K_{\mathrm{CH_4}}\mu, \tag{2}$$

where $K_{\mathrm{CH_4}}$ is the diagonal matrix whose coefficients are the ones of the methane absorption spectrum.

The methane absorption spectrum is obtained from the Hitran database [13]. The parameters μ and Σ are computed with their empirical estimates.

A major drawback of the matched filter is that we can detect anomalies that are not in the direction of the target vector if there are outliers. In our case the values of $\mathbf{t}$ are negative so for example if x has its values very close to 0 we will get a very high matched filter score, independently of the shape of the spectrum of x. This often happens when we have an area with a very low albedo, such as buildings, roads or water bodies. To avoid false positives, we need to penalize the score of these outliers, which correspond to anomalies in any direction, by using an adjusted spectral matched filter (ASMF) [4].

To penalize the anomalies that are not in the direction of the target vector we use the Reed-Xiaoli (RX) detector $\mathcal{D}_{RX}$, which can also be seen as the squared of the Mahalanobis

distance. It is defined by

$$\mathcal{D}_{RX}(x) = (x-\mu)^T \Sigma^{-1}(x-\mu). \tag{3}$$

The Reed-Xiaoli detector will return a high score for any pixel that is dissimilar to μ. The AMSF detector is then defined by [4]:

$$\mathcal{D}_{ASMF}(x) = \mathcal{D}_{MF}(x) \cdot \left(\frac{\mathcal{D}_{MF}(x)}{\mathcal{D}_{RX}(x)} \right)^2. \tag{4}$$

The ASMF significantly reduces the number of false positives. However, it can lower the detection score of actual plumes because plumes can also have a high RX score. The detection of the plumes is performed on the image resulting from the ASMF also referred to as the ASMF image. The ASMF image is centered and normalized so that the distribution of the pixels is a standard normal distribution. Then, a threshold is set on a quantile of the distribution. To prevent the detection of isolated false positives, we only keep the detections of groups of at least 3 pixels. Since the spatial resolution of PRISMA is 30m, the plumes we aim to detect will always extend over more than a hundred meters. Smaller plumes have a very low methane concentration and are therefore generally impossible to detect with the spatial and spectral resolution of PRISMA.

4.2. Wind orientation test

To validate the detections obtained with the method described above, the spatial inclination of the plume is compared with the wind direction. The wind data are obtained from the ECMWF ERA5 dataset. We interpolate the wind data closest to the mean coordinates of the plume to obtain the wind angle θ_{wind}. To calculate the plume angle θ_{plume} we perform a principal component analysis on the centered coordinates of the plume. The coordinates are centered to ignore the position of the plume in the image. The orientation of the plume is then given by the principal component.

Once θ_{wind} and θ_{plume} are computed, the two angles are compared to confirm the presence of the plume. Since the wind data is obtained up to 30min after or before the plume emission, a large margin of error must be left on θ_{wind} which may have changed. We therefore allow an error of plus or minus 30 degrees on the wind angle. If $\theta_{plume} \in [\theta_{wind} - 30, \theta_{wind} + 30]$, we consider that the plume is directed in the direction of the wind.

The shape of some plumes does not necessarily correspond to the wind direction. This can be due to weak wind conditions or to the local topography. Therefore, the wind direction information can only be used when the wind is strong enough. In particular, the plume can have a shape very close to a circle, which prevents the correct calculation of its orientation. The orientation test is only performed when the orientation of the plume is clear and when the wind is strong enough. The orientation is clear when the variance in the principal component direction is much larger than the variance in the orthogonal direction. To see if a plume is eligible for the orientation test, the ratio of the variances is calculated. The wind is considered to be strong enough when its speed is above 2.4m/s. When the ratio is large enough and the wind is above the 2.4m/s threshold, the orientation test is performed.

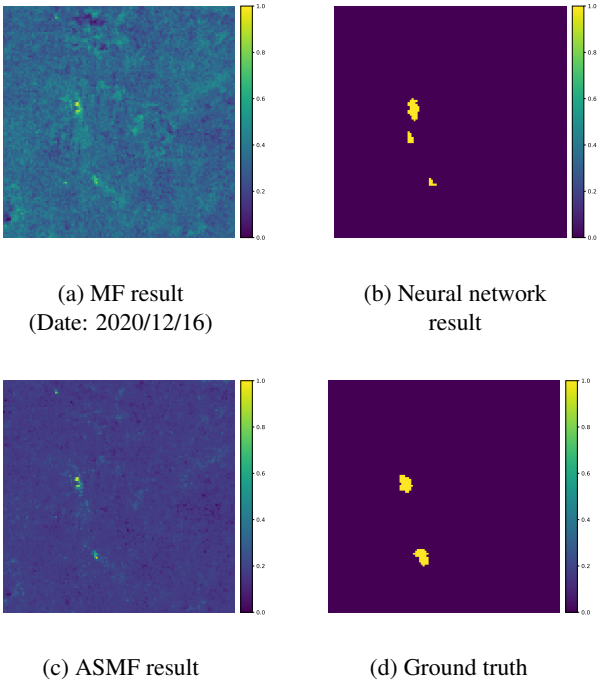

(a) MF result (Date: 2020/12/16)

(b) Neural network result

(c) ASMF result

(d) Ground truth

Fig. 2: Comparison between the Matched Filter, the deep learning method proposed by [5] and the ASMF. The different methods are here tested on a plume in Australia.

4.3. Results

As it can be seen in Figure 1 and Figure 2, the ASMF significantly improves the contrast of the plumes compared to the background. This can be seen in two main ways. First, we observe that the average background value is substantially lower with ASMF than with the MF. Also, we observe a reduction of potential false positives. This can be seen in Figure 1 with the very bright pixels on the top and the bottom of the MF image. In particular, the potential false positives on the top of the image are almost merged with the background in the ASMF image. Figure 1 also shows an example of an application of the wind orientation test. The ASMF has not completely eliminated the false positive at the bottom of the image. However, the orientation of this false positive is very different from the one of the plume and therefore also very different from the wind orientation. Thus, the wind orientation test removes the false positive.

We also compare the ASMF with the deep learning

	Recall	Precision	F1
MF [3]	0.53	0.22	0.31
Deep learning [5]	**0.88**	0.42	0.57
ASMF + wind orientation test	0.83	**0.62**	**0.71**

Table 1: Numerical results using the dataset built by [5]. The method proposed here is refered as ASMF+network

method proposed in [5]. Figure 2 shows the results of the ASMF and the deep learning method on the same plume. It can be seen that both methods bring out the plume. However, with the deep learning network, a false positive appears, which does not appear on the matched filter or ASMF results.

To confirm the improvement brought by the joint use of the ASMF and wind data we can look at Table 1 which summarizes the scores of the different methods. All methods were tested with automatic detection without manual correction. The images used are those of the dataset proposed by [5], which have been manually labeled.

The results presented in Table 1 confirm the improvement brought by our method. Indeed, the ASMF+wind orientation test method outperforms the others in terms of precision and F1 score. We can notice that it is slightly behind the deep learning method in terms of recall but this loss in recall is compensated by a significant gain in precision.

5. CONCLUSION

We have introduced an automatic methane plume detection method based on a variant of the matched filter and the use of wind data. It outperforms pre-existing methods in terms of precision and F1 score. The algorithm presented here has been tested on PRISMA satellite images. Since the characteristics of PRISMA are very close to those of other instruments such as EnMap or EMIT, we could consider extending the method to images obtained with these instruments.

6. REFERENCES

[1] Paola Arias et al., *Climate Change 2021: The Physical Science Basis. Contribution of Working Group I to the Sixth Assessment Report of the Intergovernmental Panel on Climate Change*, pp. 33–144, Cambridge University Press, 2021.

[2] Sergio Cogliati et al., "The prisma imaging spectroscopy mission: overview and first performance analysis," *Remote Sens Environ.*, vol. 262, pp. 112499, 09 2021.

[3] Luis Guanter et al., "Mapping methane point emissions with the prisma spaceborne imaging spectrometer," *Remote Sens Environ.*, vol. 265, pp. 112671, 2021.

[4] Lianru Gao et al., "Adjusted spectral matched filter for target detection in hyperspectral imagery," *Remote Sensing*, vol. 7, no. 6, pp. 6611–6634, 2015.

[5] Alexis Groshenry et al., "Detecting methane plumes using prisma: Deep learning model and data augmentation," 2022.

[6] Clive D. Rodgers, "Retrieval of atmospheric temperature and composition from remote measurements of thermal radiation," *Reviews of Geophysics*, vol. 14, pp. 609–624, 1976.

[7] Andrew Thorpe et al., "Retrieval techniques for airborne imaging of methane concentrations using high spatial and moderate spectral resolution: application to aviris," *Atmos. Meas. Tech. Discuss*, vol. 6, 09 2013.

[8] Sudhanshu Pandey et al., "Satellite observations reveal extreme methane leakage from a natural gas well blowout," *PNAS*, vol. 116, no. 52, pp. 26376–26381, Dec. 2019.

[9] André Butz et al., "Tropomi aboard sentinel-5 precursor: Prospective performance of ch4 retrievals for aerosol and cirrus loaded atmospheres," *Remote Sens Environ.*, vol. 120, no. SI, pp. 267–276, 2012.

[10] Christopher C. Funk et al., "Clustering to improve matched filter detection of weak gas plumes in hyperspectral thermal imagery," *EEE Trans Geosci Remote Sens*, vol. 39, pp. 1410 – 1420, 08 2001.

[11] Andrew K. Thorpe et al., "High resolution mapping of methane emissions from marine and terrestrial sources using a cluster-tuned matched filter technique and imaging spectrometry," *Remote Sens Environ.*, vol. 134, pp. 305 – 318, 2013.

[12] Hans Hersbach et al., "The era5 global reanalysis," *Quarterly Journal of the Royal Meteorological Society*, vol. 146, no. 730, pp. 1999–2049, 2020.

[13] Iouli E. Gordon et al., "The HITRAN2016 molecular spectroscopic database," *J Quant Spectrosc Ra*, vol. 203, pp. 3 – 69, Dec. 2017.

[14] James Theiler and Brendt Wohlberg, "Detection of unknown gas-phase chemical plumes in hyperspectral imagery," in *Algorithms and Technologies for Multispectral, Hyperspectral, and Ultraspectral Imagery XIX*, Sylvia S. Shen and Paul E. Lewis, Eds., 2013.